To appear in IEEE Explore

A DISTRIBUTED SMART PEV CHARGING ALGORITHM BASED ON FORECASTED MOBILITY ENERGY DEMAND

Mithat C. Kisacikoglu[1], *Fatih Erden*[2], *Nuh Erdogan*[2,3]

[1] Department of Electrical and Electronics Engineering, Hacettepe University, Ankara 06800, Turkey
[2] Department of Electrical and Electronics Engineering, Atilim University, Ankara 06836, Turkey
[3] Department of Electrical Engineering, University of Texas at Arlington, Arlington, Texas, 76010 USA

ABSTRACT

This study proposes a new distributed control strategy for the grid integration of plug-in electric vehicles. The proposed strategy consists of two stages: (i) an offline process to determine an aggregated reference charge power level based on mobility estimation and base load profile, and (ii) a real-time operation based on the distributed control approach. The control algorithm manages PEV charge load profiles in order to flatten the residential distribution transformer loading while ensuring the desired state of the charge (SOC) level. The proposed algorithm is tested on real distribution transformer loading data, and compared with heuristic charging scenarios. The numerical results are presented to demonstrate the impact of the proposed algorithm.

Index Terms— Plug-in electric vehicle, grid integration, peak shaving, smart charging, distributed control.

1. INTRODUCTION

Growing number of plug-in electric vehicles (PEVs) in the market is becoming a matter of concern due to the utility grid integration, especially at the distribution level [1–3]. The integration of PEVs into the distribution system with an uncoordinated fashion at high market rates increases peak loading on line/transformer, energy losses, voltage deviations, and the need for network reinforcements [1, 2, 4, 5]. When considering a cost-efficient solution for both the utility grid and PEV user, it is more convenient to shift PEV charging loads to off-peak hours where the demand load and the electricity price is lower. However, shifting PEV loads with uncoordinated charging strategies imposes a non-uniform load profile, resulting in undesired peak loads at off-peak hours due to the charging many PEVs simultaneously [6].

The peak loads caused by PEV charging can be restrained either by unidirectional PEV charging management [4, 6] or by discharging PEV batteries into the grid using vehicle-to-grid (V2G) technology [7, 8]. V2G requires special hardware allowing bidirectional power transfer, which is currently not available in the most of the market vehicles yet. Also, the lack of an established electric vehicle grid integration (EVGI) protocol and market agreement make it difficult to provide field deployment for mass V2G technologies [9]. Therefore, coordinated unidirectional charging becomes prominent for large-scale penetration of PEVs into the grid in the near-term.

Coordinated charging manages PEV charging loads effectively to mitigate largely undesirable impacts of high penetration of PEVs in the grid [4,5]. It enables a charging flexibility which can be used to provide grid services such as peak shaving [6], valley filling [10], and minimizing charging cost [11]. It can also be used to integrate higher share of intermittent renewable energy sources into the grid [12]. Centralized [13, 14] and distributed (decentralized) [10,11,13,15,16] charging strategies have been proposed in the literature. While charging profile for each PEV in the centralized strategy is managed by a central operator which aims to achieve an optimal aggregated charging goal, the distributed strategy allows each PEV to determine its own charging profile which may not always result in optimal aggregated charging regime [11]. The distributed approach has gained more attraction in the literature because of its higher flexibility to the PEV user and easier field implementation [10, 11, 13, 15, 16]. However, issues in terms of better utility grid coordination while considering PEV user convenience at the same time is still an undergoing research topic.

This study contributes to the integration of PEVs into the distribution system by proposing a distributed smart charging algorithm. The proposed algorithm minimizes the peak loading on the distribution system, fills the night-valley as much as possible while ensuring the desired state of charge (SOC) level, i.e. full-charging, at departure time. In contrast to the charging at constant rated power proposed in [10, 13, 15, 16], charging process for each PEV is performed at variable power rates to achieve better valley filling performance. To achieve this, a new two-stage control approach is presented. First, an offline process is proposed to determine the charge reference which is estimated using PEV mobility data and base load profile. In the second phase of the control mechanism, a real-time operation based on the distributed control approach is carried out. The algorithm not only provides an optimal aggregated load profile based on the objective of minimizing its

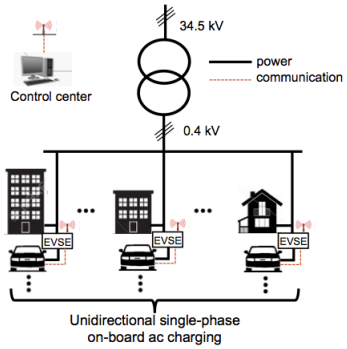

Fig. 1. EVGI architecture in the distribution system.

Table 1. Types of PEVs and Their Specifications

Vehicle Make and Model	Vehicle Type	Battery Size (kWh)	EV Range (km)	Max. charge power (kW)
BMW i3	EV	18	110	7.4
Chevy Volt	PHEV	10	50	3.3
Nissan Leaf	EV	24	150	6.6
Renault Zoe	EV	22	100	7.4
Tesla Model S	EV	85	350	10

variance, but also utilizes the advantages of distributed strategy, i.e. retaining PEV user private information and avoiding the communication and computation overhead. The proposed algorithm is tested on real distribution transformer loading data, and compared with heuristic charging scenarios. The performance of the algorithm is quantified in terms of variance and mean square error metrics.

2. SYSTEM DESCRIPTION AND MODELING

In this study, system modeling is done in MATLAB Simulink through off-line and time-based simulation environments. The described system architecture is demonstrated in Fig. 1. The components of the system model are individually described in the below sections.

2.1. Transportation Mobility Modeling

Daily home arrival/departure time and trip distance data of 10 personal vehicles have been collected for a year to constitute a realistic mobility model [17]. The collected data histograms are quite similar to a Gaussian distribution with mean and standard deviations of (7h47, 0h23), (19h55, 1h40), and (39.5 km, 15.8 km) for home departure time, arrival time, and daily trip distance distributions, respectively. Five different PEVs listed in Table 1 are randomly selected in the model. The transportation model runs off-line and generates SOC values for individual PEVs at the time of grid connection.

2.2. Charging Station Model

Charging station (electric vehicle supply equipment- EVSE) model includes a user behavior model which is classified as follows:

i-)Standard charging: PEV charges at rated on-board charging power when connected to the grid. No control over charging is possible. Charging ends when the PEV is fully charged.

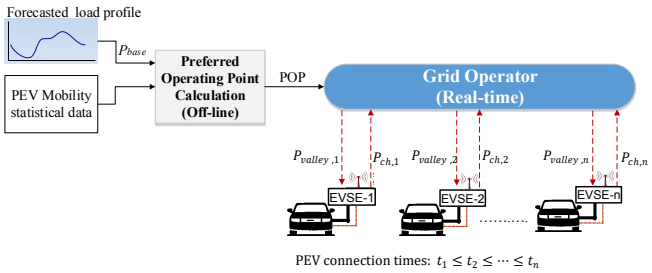

Fig. 2. Structure of proposed smart charging algorithm.

ii-)Smart charging: PEV starts charging with a smart charging profile during the time when the system loading is below a certain reference value. Charging ends in the morning departure time with fully charged battery.

The EVSE communicates with the control center using a wireless/wired set-up. Vehicle - station communication is employed through the low-level and high-level communication over the control pilot. The related high-level vehicle information can be transferred between the EVSE and the PEV through power line communication over the control pilot pin utilizing standards such as ISO15118 or Homeplug Green PHY [18].

2.3. On-board Charger and Battery System Model

The PEV component models are developed to simulate the AC power exchange between the vehicle and the grid. It includes the following information for different vehicle vendors: on-board charger power rating, operating efficiency, implementation of constant-current (CC) and constant-voltage (CV) charging, and cell-based battery system design.

3. DISTRIBUTED SMART CHARGING ALGORITHM

The proposed control approach consists of two phases, offline and real-time processing, as shown in Fig. 2. During the offline process, a charge reference called preferred operation point (POP) is determined. In the second phase, a real-time operation based on the distributed control approach is carried out. The following operations are performed when each PEV is connected to the grid. (i) The grid operator sends the valley power profile to i^{th} PEV connected to the grid; (ii) the PEV independently determines its own charging profile depending on the valley energy, its SOC, and morning departure time, and then sends it to the grid operator; (iii) the grid operator updates valley power and send it to $(i+1)^{th}$ PEV connected to the grid. The algorithm repeats the second and third steps whenever a new PEV connects to the grid.

Offline operation: The output of this stage is to estimate a POP value as a reference for the aggregated charging of all PEVs. For this to be achieved, the total number of PEVs in the region and their types (makes/models) are known ahead. Then, the energy for each PEV to be fully charged before the

time of departure is calculated. To do so, a mobility data set (daily distances taken, home arrival and departure times) is generated based on the pre-determined Gaussian characteristics described in Section II. Later, by considering the battery capacities of each PEV and the distances taken by that PEV, required energy for an SOC level of 100% is computed. As a final step, POP value is decided based on the total required energy in an iterative manner. Valley energy is defined as follows:

$$E_{valley} = \int_{t_{arr,1}}^{t_{dept,ave}} P_{valley}(t)dt, \quad (1)$$

where,

$$P_{valley}(t) = \begin{cases} POP - P_{base}(t), & \text{if} \quad POP - P_{base}(t) > 0 \\ 0, & \text{otherwise} \end{cases} \quad (2)$$

and $t_{arr,1}$ is the time when the first PEV arrives home and $t_{dept,ave}$ is the average of the departure times of all PEVs. The valley energy is compared to the required energy and POP value is increased/decreased accordingly. Iterations are stopped when a convergence criteria is satisfied. To have a good representation of a global POP value, the above procedure is repeated 100 times and the mean of the all POP values are used as the final forecasted POP value.

Online operation: Once the POP value is calculated, the only information to be transferred to PEVs to determine the charging profile for each PEV is the $P_{valley}(t)$ which is calculated using (2). To determine the charging power of a PEV at time t, the valley energy for that PEV is calculated first:

$$E_{valley,i}(t) = \int_{t}^{t_{dept,i}} P_{valley}(\tau)d\tau, \quad t_{arr,i} < t < t_{dept,i} \quad (3)$$

where, $t_{arr,i}$ is the arrival time and $t_{dept,i}$ is the departure time of the i^{th} PEV. Then, a multiplication factor, $\alpha(t)$, is computed as:

$$\alpha_i(t) = \begin{cases} \dfrac{E_{rated,i} \times (1 - SOC_i(t))}{E_{valley,i}(t)}, & \text{if } t_{arr,i} < t < t_{dept,i} \\ 0, & \text{otherwise} \end{cases} \quad (4)$$

where $E_{rated,i}$ is the rated battery capacity of the i^{th} PEV. Finally the charging power for the i^{th} PEV at time t is

$$P_{ch,i}(t) = \alpha_i(t) \times P_{valley}(t). \quad (5)$$

In this study, the charging control signals for each PEV are compliant with the IEC 61851 standard which imposes that the charging current has to be at least 6 A [19]. For this purpose, if $P_{ch,i}$ in the above equation results in a value below the possible minimum charging power (1.32kW at 220 V), then it is updated as follows:

$$P_{ch,i}(t) = \begin{cases} 0 \text{ kW}, & if \quad 0 < P_{ch,i} < 0.66 \text{ kW} \\ 1.32 \text{ kW} & if \quad 0.66 \text{ kW} < P_{ch,i} < 1.32 \text{ kW} \end{cases} \quad (6)$$

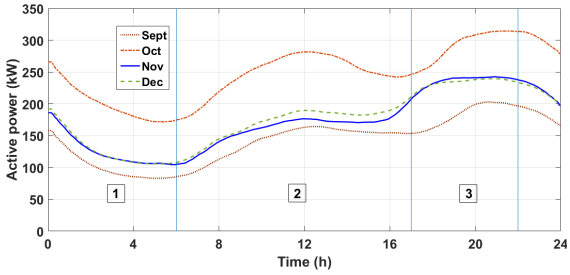

Fig. 3. Daily average active power demands for four months.

At the end of time t, $SOC_i(t)$ is updated accordingly and the above procedure is repeated between (4) and (6) to find the charging power for the same vehicle at time $t+1$. Having determined the $P_{ch,i}(t)$ for the whole time period when the i^{th} PEV is parked, this information is sent to the grid, and $P_{valley}(t)$ is updated. That is:

$$P_{valley}(t) = P_{valley}(t) - P_{ch,i}(t), \quad 0h < t < 24h \quad (7)$$

The charging power for subsequent PEV connected to the grid is determined based on this new value of the valley power.

Highlights of the proposed control approach: The control approach has several advantages in terms of computational complexity, communication overhead, and practicability for real-time application, resulting from the distributed control approach. Since the charging calculations are distributed to PEVs, the computational overhead is avoided. Moreover, the charging profile for each PEV is determined in a non-iterative manner that decreases the communication rate. It is calculated only once when the PEV connects to the grid and it does not need to be updated depending on the other PEVs arriving later than that PEV. From PEV user privacy perspective, the control approach preserves user private data since PEVs report only charging profiles. The solutions of the charging profile expressions do not require an extensive calculation. The charging expressions can be easily solved by an embedded system in each PEV/EVSE. Therefore, the control approach is quite appropriate for field implementation.

4. CASE STUDIES AND RESULTS

The case studies are developed using the distribution network of city of Ankara in Turkey. A three-phase distribution transformer of 34.5/0.4 kV, 1000 kVA, with 985 residential customers are used. The daily average active power profile during four months are shown in Fig. 3. Among the available months, November is chosen as the forecasted daily power consumption. The triple tariff regions (1, 2, and 3) shown in the figure correspond to night (10 pm - 6 am), day-time (6 am - 5 pm) and peak-time (5 pm - 10 pm) hours, respectively. The proof of concept is demonstrated for the PEV penetration level of 10%. This corresponds roughly to 100 vehicles for 985 customers in the neighborhood assuming each household owns one vehicle.

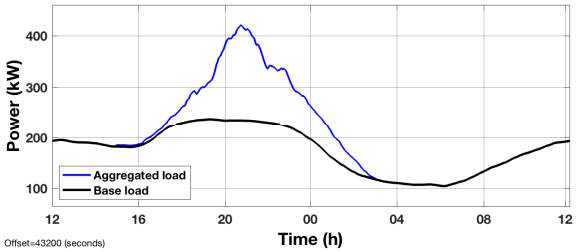

Fig. 4. Result of 10% PEV penetration for Case 1.

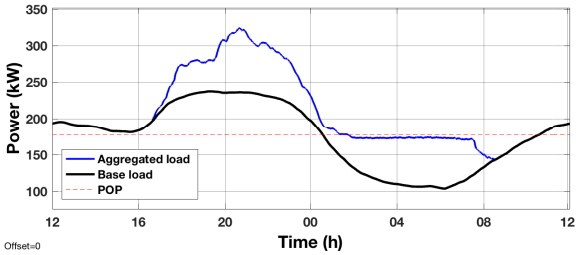

Fig. 5. Result of 10% PEV penetration for Case 2.

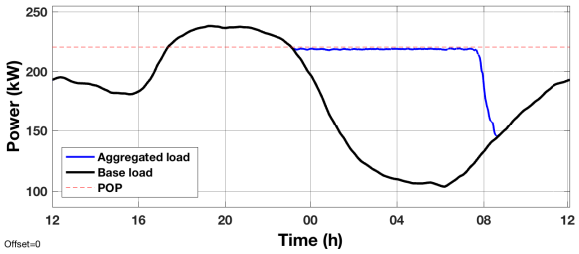

Fig. 6. Result of 10% PEV penetration for Case 3.

Three different cases have been tested to evaluate the algorithm performance. Fig. 4 shows the loading result of Case 1 where all PEVs are charged at their rated charging power as they arrive without any coordination. As shown, the peak of the aggregated load has considerably increased as opposed to base loading (almost two-fold). Meanwhile, Fig. 5 shows the result of Case 2 where only half of the PEVs are charged in coordination with the smart charging profile. The POP value for this case is calculated off-line to be 177 kW. Finally, Fig. 6 shows the result of Case 3 where all of the PEVs obey coordinated charging. The POP value for this case is 220 kW. As shown, there is no increase on the base peak power loading of the transformer. In order to evaluate and compare the operation results, variance is used as the base metric. Minimizing the variance shows how well the algorithm smooths the aggregated load profile helping for the better utilization of the power generation assets. The variance is calculated as follows:

$$v = \frac{1}{t_{dept,ave} - t_{arr,ave}} \sum_{t=t_{arr,ave}}^{t_{dept,ave}} (P_{aggr}(t) - \mu)^2, \quad (8)$$

where $P_{aggr}(t)$ and μ are the aggregated and the average loading profiles (kW), respectively. The calculations are done in one-minute intervals during the time horizon when vehicles are parked and grid connected at home. The average arrival and departure times of the vehicle set are $t_{arr,ave}$=7:55 pm and $t_{dept,ave}$=7:47 am. According to Table 2, the case with the lowest variance (Case 3) returns the best overall utilization of the generation sources without causing high demand charges for the utility operator. In contrast, Case 1 returns the worst utilization of the assets. As the number of PEVs participating into smart charging service increases, the variance of the aggregated loading decreases. For all three cases, PEV user convenience is met by providing a fully charged PEV battery in the morning departure.

Table 2. Different Test Cases

Case #	Standard charging PEVs [%]	Smart charging PEVs [%]	MSE* $(kW)^2$	Variance† $(kW)^2$
1	100	0	N/A	12405
2	50	50	17.4	3304
3	0	100	1.9	51.7

*Calculated between 1:00 am and 7:00 am.

†Calculated between 7:55 pm and 7:47 am next day.

As a second measure, mean-square-error (MSE) is also used. It is a measure of how close the aggregated loading profile is to the expected charge reference (POP value). This metric can be used when a PEV aggregator promises to provide a load consumption service to the utility grid in a predefined time interval, i.e. t_1=1:00 am to t_2=7:00 am. The MSE can be computed as follows:

$$MSE = \frac{1}{t_2 - t_1} \sum_{t=t_1}^{t_2} (P_{aggr}(t) - POP)^2. \quad (9)$$

The algorithm performance is better for Case 3 compared to Case 2 in the MSE calculation as shown in Table 2. Overall, the proposed control algorithm handles EVGI impact on the distribution system for different user choices successfully and provides a smooth and constant loading profile by selecting a corresponding charging reference to be followed by the PEVs.

5. CONCLUSION

A smart charging algorithm to smoothen the load profile on the residential distribution transformer has been presented in this paper. A new distributed-based smart charging control algorithm has been developed by addressing PEV user convenience and practicability in real-time applications. The proposed algorithm avoids computational overhead, decreases the communication rate, and retains PEV user private data. The algorithm has been tested on a real residential transformer data with heuristic charging scenarios. It is shown that the proposed algorithm reduces the peak loading resulting from the mass PEV charging, and performs a significant valley-filling performance without extensive centralized controller requirements.

6. REFERENCES

[1] L. P. Fernandez, T. G. S. Roman, R. Cossent, C. M. Domingo, and P. Frias, "Assessment of the impact of plug-in electric vehicles on distribution networks," *IEEE Trans. Power Syst.*, vol. 26, no. 1, pp. 206–213, Feb 2011.

[2] S. Shafiee, M. Fotuhi-Firuzabad, and M. Rastegar, "Investigating the impacts of plug-in hybrid electric vehicles on power distribution systems," *IEEE Trans. Smart Grid*, vol. 4, no. 3, pp. 1351–1360, Sept 2013.

[3] E. Veldman and R. A. Verzijlbergh, "Distribution grid impacts of smart electric vehicle charging from different perspectives," *IEEE Trans. Smart Grid*, vol. 6, no. 1, pp. 333–342, 2015.

[4] E. Sortomme, M. M. Hindi, S. D. J. MacPherson, and S. S. Venkata, "Coordinated charging of plug-in hybrid electric vehicles to minimize distribution system losses," *IEEE Trans. Smart Grid*, vol. 2, no. 1, pp. 198–205, March 2011.

[5] N. Leemput, F. Geth, J. V. Roy, A. Delnooz, J. Bscher, and J. Driesen, "Impact of electric vehicle on-board single-phase charging strategies on a flemish residential grid," *IEEE Trans. Smart Grid*, vol. 5, no. 4, pp. 1815–1822, July 2014.

[6] A. S. Masoum, S. Deilami, P. S. Moses, M. A. S. Masoum, and A. Abu-Siada, "Smart load management of plug-in electric vehicles in distribution and residential networks with charging stations for peak shaving and loss minimisation considering voltage regulation," *IET Generation, Transmission Distribution*, vol. 5, no. 8, pp. 877–888, August 2011.

[7] Z. Wang and S. Wang, "Grid power peak shaving and valley filling using vehicle-to-grid systems," *IEEE Trans. Power Del.*, vol. 28, no. 3, pp. 1822–1829, July 2013.

[8] M. C. Kisacikoglu, M. Kesler, and L. M. Tolbert, "Single-phase on-board bidirectional PEV charger for V2G reactive power operation," *IEEE Trans. Smart Grid*, vol. 6, no. 2, pp. 767–775, March 2015.

[9] M. C. Kisacikoglu, T. Markel, A. Meintz, J. Zhang, and M. Jun, "EV-grid integration (EVGI) control and system implementation-research overview," presented at the IEEE Applied Power Electron. Conf. Expo. (APEC), March 2016.

[10] G. Binetti, A. Davoudi, D. Naso, B. Turchiano, and F. L. Lewis, "Scalable real-time electric vehicles charging with discrete charging rates," *IEEE Trans. Smart Grid*, vol. 6, no. 5, pp. 2211–2220, Sept 2015.

[11] Z. Ma, D. S. Callaway, and I. A. Hiskens, "Decentralized charging control of large populations of plug-in electric vehicles," *IEEE Trans. Control Syst. Technol.*, vol. 21, no. 1, pp. 67–78, Jan 2013.

[12] T. Wu, Q. Yang, Z. Bao, and W. Yan, "Coordinated energy dispatching in microgrid with wind power generation and plug-in electric vehicles," *IEEE Trans. Smart Grid*, vol. 4, no. 3, pp. 1453–1463, Sept 2013.

[13] C. K. Wen, J. C. Chen, J. H. Teng, and P. Ting, "Decentralized plug-in electric vehicle charging selection algorithm in power systems," *IEEE Trans. Smart Grid*, vol. 3, no. 4, pp. 1779–1789, Dec 2012.

[14] A. Di Giorgio, F. Liberati, and S. Canale, "Electric vehicles charging control in a smart grid: A model predictive control approach," *Control Engineering Practice*, vol. 22, pp. 147–162, 2014.

[15] A. Malhotra, G. Binetti, A. Davoudi, and I. D. Schizas, "Distributed power profile tracking for heterogeneous charging of electric vehicles," *IEEE Trans. Smart Grid*, vol. PP, no. 99, pp. 1–10, 2016.

[16] Q. Li, T. Cui, R. Negi, F. Franchetti, and M. D. Ilic, "On-line decentralized charging of plug-in electric vehicles in power systems," *arXiv preprint arXiv:1106.5063*, 2011.

[17] F. Erden, M. C. Kisacikoglu, and O. H. Gurec, "Examination of EV-grid integration using real driving and transformer loading data," in *9th International Conference on Electrical and Electronics Engineering*, Nov. 2015.

[18] "Road vehicles-vehicle to grid communication interface," *ISO/IEC Standard 15118*, 2013.

[19] I. E. Comission, "Electric vehicle conductive charging system- part-i: General requirements," *Standard 61851-1*, 2010.